
14 Feb 2013

Carbothermal Synthesis of Titanium Oxycarbide as Electrocatalyst Support with High Oxygen Evolution Reaction Activity

Kan Huang

Yunfeng Li

Yangchuan Xing

Missouri University of Science and Technology, XingY@Missouri.edu

Follow this and additional works at: https://scholarsmine.mst.edu/che_bioeng_facwork



Part of the [Biochemical and Biomolecular Engineering Commons](#)

Recommended Citation

K. Huang et al., "Carbothermal Synthesis of Titanium Oxycarbide as Electrocatalyst Support with High Oxygen Evolution Reaction Activity," *Journal of Materials Research*, vol. 28, no. 3, pp. 454 - 460, Springer; Materials Research Society, Feb 2013.

The definitive version is available at <https://doi.org/10.1557/jmr.2012.353>

This Article - Journal is brought to you for free and open access by Scholars' Mine. It has been accepted for inclusion in Chemical and Biochemical Engineering Faculty Research & Creative Works by an authorized administrator of Scholars' Mine. This work is protected by U. S. Copyright Law. Unauthorized use including reproduction for redistribution requires the permission of the copyright holder. For more information, please contact scholarsmine@mst.edu.

Carbothermal synthesis of titanium oxycarbide as electrocatalyst support with high oxygen evolution reaction activity

Kan Huang and Yunfeng Li

Department of Chemical and Biological Engineering, Missouri University of Science and Technology, Rolla, Missouri 65409

Yangchuan Xing^{a)}

Department of Chemical Engineering, University of Missouri, Columbia, Missouri 65211

(Received 7 May 2012; accepted 21 September 2012)

Carbothermal reduction of semiconducting TiO₂ into highly conductive titanium oxycarbide (TiO_xC_y) was investigated. The thermally produced uniform carbon layer on TiO₂ (Degussa P25) protects the TiO₂ nanoparticles from sintering and, at the same time, supplies the carbon source for doping TiO₂ with carbon. At low temperatures (e.g., 700 °C), carbon only substitutes part of the oxide and distorts the TiO₂ lattice to form TiO_{2-x}C_x with only substitutional carbon. When the carbon-doped TiO₂ is annealed at a higher temperature (1100 °C), x-ray diffraction and x-ray photoelectron spectroscopy results showed that TiO_xC_y, a solid solution of TiO and TiC, was formed, which displays different diffraction peaks and binding energies. It was shown that TiO_xC_y has much better oxygen evolution reaction activity than TiO₂ or TiO_{2-x}C_x. Further studies showed that the TiO_xC_y obtained can be used as a support for metal electrocatalyst, leading to a bifunctional catalyst effective for both oxygen reduction and evolution reactions.

I. INTRODUCTION

Carbon black has for a long time served as electrocatalyst support for porous electrodes in fuel cells and metal–air batteries.^{1–7} These carbon particles contribute as reaction sites for the oxygen reduction reaction (ORR) or oxygen evolution reaction (OER), especially during discharge and recharge processes. However, the fact of severe corrosion of carbon materials at high potentials during electrochemical reactions⁸ makes such applications impractical under long-term cell operation in acidic media.⁹ Therefore, alternative catalyst supports have to be sought, and recent attention has been focused on TiO₂ as a stable support candidate.^{10–12} Due to the semiconducting nature of TiO₂, great efforts were taken to improve its electronic conductivity.

One type of reduced TiO₂, called Magneli phase (Ti_xO_{2x-1}), has been shown to have high stability and electron conductivity in corrosive electrolytes and at high potentials.^{13–16} Yet, the reduction condition for making the Magneli phase is generally rather harsh, requiring very high temperatures under hydrogen, leading to severe sintering and consequently significant loss of surface areas. On the other hand, carbon-modified anatase TiO₂ nanoparticles and nanotube arrays under relatively mild conditions have been demonstrated to be effective in photocatalysis and applied in dye-sensitized solar cells.^{17–21} The TiO₂ carbon modification methods include carbon

monoxide reduction,²⁰ acetylene reduction,²² flame made with TiC,^{19,23} or polymer TiO₂ composites.^{17,24} X-ray photoelectron spectroscopy (XPS) results of these samples revealed the presence of carbon in all of them.²¹ However, the particle size distributions obtained by these processes are rather broad.^{25,26}

Carbon coating has been reported to suppress sintering of TiO₂ during high temperature annealing.^{17,22,24} The technique could allow tuning the nanoparticle TiO₂ electronic conductivity while maintaining its high surface areas, making it possible to obtain titanium oxycarbide (TiO_xC_y), which can be viewed as a solid solution of TiO in TiC and various titanium suboxides (TiO_x, $x < 2$).²⁷ For example, Hahn et al.²⁷ have reported TiO₂ arrays that were converted into TiO_xC_y with high conductivity and stability during redox cycles. Carbothermal techniques have been widely used to make metal carbide from metal oxide. The current work aims at making nanoscale TiO_xC_y in a carbothermal process from Degussa P25, which is commercially and cheaply available.

To date, it is quite common that platinumized TiO₂ were reported as catalysts in the field of photocatalysis.^{28,29} Also, those active components for OER in bifunctional electrocatalysts in regenerative fuel cells are normally precious metals or their oxides, such as Ir or IrO₂.^{30,31} However, there is not much literature on such electronically conductive TiO₂ as the substrate for loading Pt electrocatalyst for ORR but also active for OER. Herein, we report a carbothermal reduction technique to convert P25 TiO₂ nanoparticles into nanoscale TiO_xC_y in a one-step two-stage

^{a)}Address all correspondence to this author.

e-mail: xingy@missouri.edu

DOI: 10.1557/jmr.2012.353

process. It is shown that the carbon-modified TiO_2 has a narrow size distribution. Their sizes increased but remain small at less than 50 nm, even annealed at 1100 °C. Electrochemical characterizations revealed that the obtained TiO_xC_y is a very active OER catalyst. Together with Pt, the catalyst is bifunctional, good for both ORR and OER.

II. EXPERIMENTAL

Amorphous TiO_2 powders (P25; Degussa Corp., Germany) with a mean size at 22 nm were thermally coated with carbon under 10% acetylene C_2H_2 in N_2 for 20 min at 700 °C in a tubular quartz furnace. After carbon coating, the products were further annealed under 10% H_2 in N_2 between 900 and 1100 °C for another 4 h. The samples were designated as P25-700 for the thermally coated TiO_2 at 700 °C and P25-700-1100h for the annealed and carbon-doped TiO_2 at 1100 °C. The latter notation is also referred to c- TiO_2 . Pt (10 wt%) loaded on the samples for electrochemical measurements was achieved using a salt reduction method reported previously.³²

The morphologies of the powders were examined by transmission electron microscope (TEM) (Tecnai F20, FEI, Hillsboro, OR) operating at 300 kV and scanning electron microscope (SEM) (Helios NanoLab 600, FEI, Hillsboro, OR) operating at 30 kV. The crystalline phase of the catalysts was analyzed by x-ray diffraction (XRD) equipped with $\text{Cu K}\alpha$; the XRD data were collected with a Philips X'Pert Diffractometer (Netherlands). XPS (Kratos Axis 165, Japan) was used to analyze C (1s), Ti (2p), and O (1s) by using Al $\text{K}\alpha$ excitation, operated at 150 W and 15 kV.

Electrochemical techniques such as cyclic voltammetry (CV), ORR, and OER were used for testing support conductivity and measuring the electrochemical activities of the titanium oxide nanopowders. CV of 10 wt% Pt-loaded or Pt-free catalyst was carried out at a scan rate of 50 mV/s in N_2 -purged 1.0 M H_2SO_4 from 0 to 1.2 V versus reversible hydrogen electrode (RHE). All measurements were performed with a standard three-electrode cell using a glassy carbon rotating disk electrode (Pine Instruments, Grove, PA) supporting 0.02 mg catalyst as working electrode. A Pt wire was used as the counter electrode and a saturated Ag/AgCl as reference electrode. CV, OER, and durability of the catalysts were carried in a N_2 -saturated 1.0 M H_2SO_4 electrolyte solution. ORR was carried in an O_2 -saturated 1.0 M H_2SO_4 electrolyte solution.

III. RESULTS AND DISCUSSION

Figures 1(a)–1(f) show the morphologies of P25 untreated and thermally treated at different temperatures. After carbon coating process at 700 °C, the amorphous TiO_2 crystallized and the mean size grows from the original 22 nm to about 35 nm [see Fig. 1(b)]. Further annealing up to 1000 °C, the particles only yield tiny growth and are still in a range of

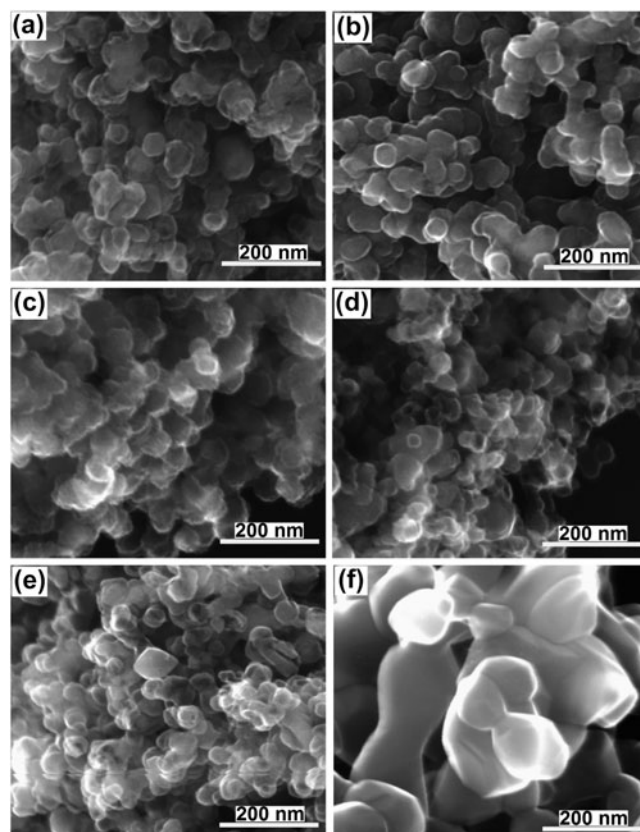


FIG. 1. SEM images of titanium oxide nanopowders obtained under different thermal treatments. (a) P25: original TiO_2 , (b) P25-700: P25 carbon coated at 700 °C, (c) P25-700-900h: P25 carbon coated at 700 °C and further annealed at 900 °C, (d) P25-700-1000h: P25 carbon coated at 700 °C and further annealed at 1000 °C, (e) P25-700-1100h: P25 carbon coated at 700 °C and further annealed at 1100 °C, and (f) P25 annealed in air at 800 °C. Annealing time was 4 h for all samples.

30–40 nm; no obvious sintering was detected and the shape of particles still appears spherical, shown in Figs. 1(c) and 1(d). When the annealing temperature was increased to 1100 °C, some particles agglomerated and their sizes increased to about 55 nm, see Fig. 1(e). A sample of P25 was directly annealed in air at 800 °C for the same duration, resulting in a substantial growth of particle size (up 300 nm), as can be seen from Fig. 1(f). It is clearly shown that the carbon nanocoating is necessary to prevent severe sintering in the TiO_2 nanoparticles.

Further investigation of these carbon-doped TiO_2 morphology by TEM revealed the reason for the suppression of particle growth. Figure 2 presents the TEM micrographs of P25-700 in Fig. 2(a) and P25-700-1100h in Fig. 2(b). The darker areas are crystalline TiO_2 particles, whose lattice spacing is shown in the inset [Fig. 2(a)], and the lighter areas surrounding the darker areas are amorphous carbon coatings with a thickness of ~5 nm. Apparently, the coating process produces an extremely uniform thin carbon on the TiO_2 surface. The TEM images also indicate that carbon existed as amorphous,

which is consistent with the XRD finding and will be further discussed below.

The carbon coating prevents the interaction of individual TiO_2 particles through surface or solid diffusion, limiting their sintering. With further annealing under N_2/H_2 at 1100°C , as shown in Fig. 2(b), the particles started to coarsen and grow. It was found that some surrounding carbon coating has disappeared. However, some free carbon still can be seen. Koc and Folmer³³ suggested that the reaction of carbon with TiO_2 only complete at above 1500°C . No further studies were conducted at higher temperatures to avoid growth.

Figure 3 shows the XRD patterns of the samples annealed at different temperatures. After carbon coating at 700°C , all peaks are related to the TiO_2 anatase or rutile phases, implying that the pyrolytic carbon formed was amorphous (no graphitic phase).^{21,34} Annealing at 900°C did not produce new phases either. However, when annealed at 1000°C , clearly, five new diffraction peaks at $2\theta \approx 37^\circ, 43^\circ, 62^\circ, 74^\circ,$ and 78° were formed,

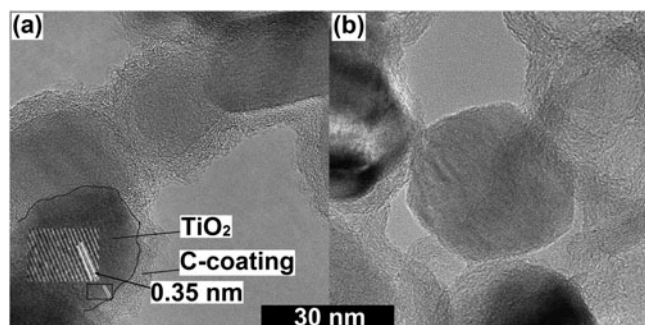


FIG. 2. TEM micrographs of (a) P25-700 and (b) P25-700-1100h, showing uniform carbon coating on the oxide nanoparticles. A contrast is observed between the amorphous carbon and the crystalline titanium oxide or oxycarbide. The inset in (a) shows the lattice spacing of TiO_2 .

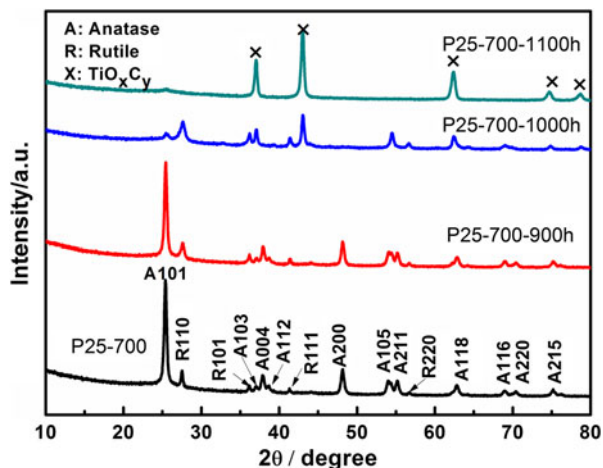


FIG. 3. XRD patterns of P25-700 and those samples annealed at 900°C , 1000°C , and 1100°C . Complete conversion to TiO_xC_y was found at 1100°C .

which all can be attributed to the formation of titanium oxycarbide (TiO_xC_y).^{27,33} As Hahn et al.²⁷ suggested, titanium oxycarbide is a solid solution of TiO in TiC and various suboxides. XPS analysis below will further support the formation of titanium oxycarbide. Increasing the temperature to 1100°C , the anatase and rutile phases disappeared completely; the TiO_xC_y peaks become shaper and well defined, which means the formation of TiO_xC_y was completed in the duration of treatment.

The chemical states of O, Ti, and C were investigated by XPS, and the results are shown in Fig. 4. Two C $1s$ peaks found at 284.6 and 285.7 eV in all powders are attributed to the carbon source from carbon tape (for sample mounting) and carbonaceous species (in sample).³⁵ No additional C $1s$ peak was found near 281.5 eV, which would correspond to TiC .³⁶ This result is indicative of that even annealing at 1100°C , the doped carbon can only interact with TiO_2 to form TiO_xC_y but not TiC . Generally, TiC can be produced by carbon reduction of TiO_2 only at 1500°C or above.³³

Figure 4(b) presents the Ti $2p$ spectra. For pure TiO_2 samples, Ti $2p_{3/2}$ and $2p_{1/2}$ peaks can be found at binding energy (BE) of 458.3 and 464.1 eV, respectively. Small peak shifts of Ti $2p$ toward higher binding energies can be observed in all samples. According to Li et al.,¹⁴ pure TiO_2 displays BEs at 464.2 and 485.5 eV, while the reduced form, Magneli phase Ti_4O_7 , has BEs at 464.7 and 459.0 eV. Göpel et al.³⁷ suggested that the shift of Ti $2p$ from defect-free TiO_2 is caused by surface oxygen vacancy defects. Carbon can be incorporated into TiO_2 lattice or substituted for oxygen, which can have synergistic effect with oxygen vacancies, resulting in the change of electronic structure between the conducting band and the valence band.³⁸ Our recent work also reported this Ti $2p$ shift.³⁹ Therefore, the Ti $2p$ shift suggests that a reduced oxide layer was formed from carbon doping. When annealing at 1100°C , a typical shoulder belonging to TiO_xC_y was detected.²⁷ This broad shoulder can be divided into several groups, titanium suboxide (TiO_x), TiO , TiC , and Ti , as Blackstock et al.⁴⁰ suggested. The Ti $2p$ spectra of the sample P25-700-1100h further consolidated our previous argument that TiO_xC_y was formed.

The O $1s$ spectra showed one peak at 529.6 eV in pure TiO_2 , which is due to the Ti-O bonding. By doping with carbon and further annealing at 1000°C , two new peaks were discovered. The peak at 529.9 eV can still be ascribed to the contribution of Ti-O bonding, even though there is a small shift. The shift may be caused by replacement of oxygen by carbon to form $\text{TiO}_{2-x}\text{C}_x$, with trace carbon distortion to the TiO_2 lattice. The other peak found at 533.6 eV can be assigned to C-O in carboxyl groups.⁴¹ When annealed at above 1000°C , the O $1s$ peak at 533.6 eV disappeared and an obvious shift was observed for the Ti-O bonding, which was also found by Hahn et al.²⁷ Both XRD and Ti $2p$ spectra have shown the formation of TiO_xC_y , and

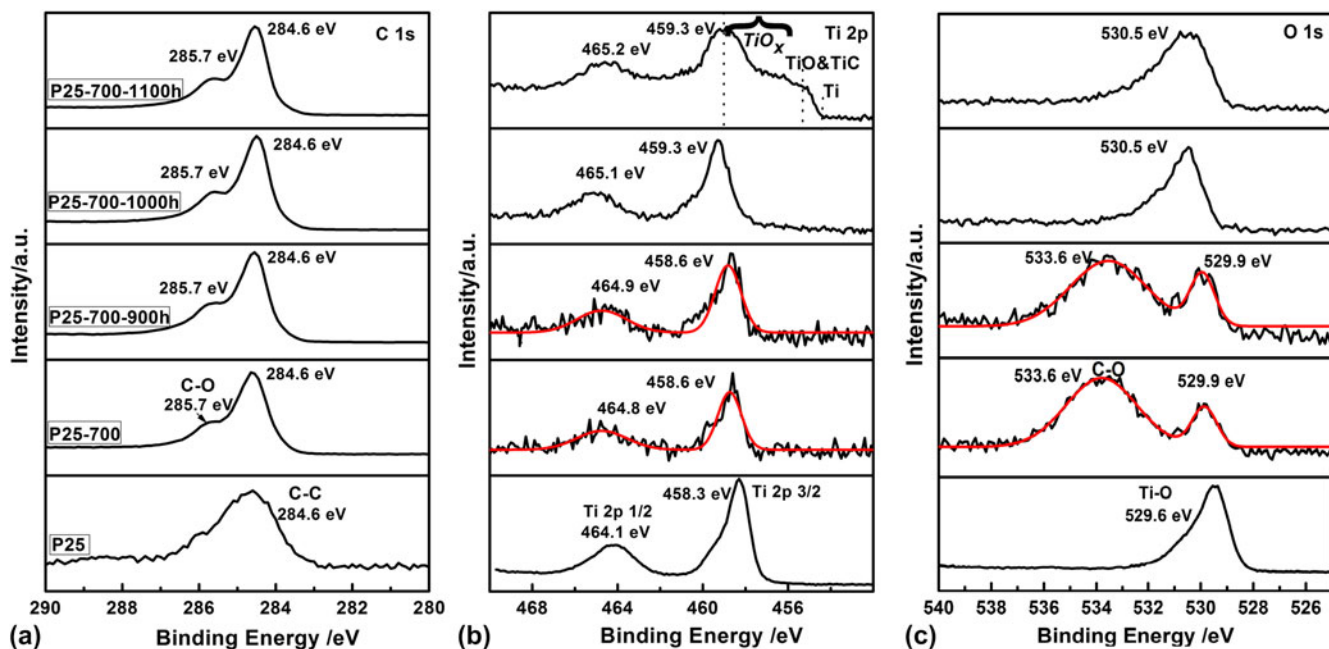


FIG. 4. XPS results of C 1s, O 1s, and Ti 2p for P25, P25-700, P25-700-900h, P25-700-1000h, and P25-700-1100h. A broad shoulder is observed in the last sample, showing formation of TiO_xC_y .

we can ascribe the O 1s at 530.5 eV to the Ti–O bonding in TiO_xC_y .

Figure 5 compares the electrochemical activity of Pt/P25 with that of Pt/P25-700. It clearly demonstrates that Pt nanoparticles supported on P25-700 exhibit much higher electrochemical activity, while Pt loaded on undoped TiO_2 shows negligible catalytic activity due to low conductivity of the support. These results demonstrate that carbon doping indeed significantly increased the electronic conductivity in P25 with carbothermal treatment. The combined effects of substitutional carbon, interstitial carbon, and oxygen vacancy contribute to the change in the band structure of TiO_2 ,³⁸ resulting in the increase of its conductivity. The close contact of Pt with its conducting support enables the catalyst to have typical Pt electrochemical activity in the CV, as displayed in the regions of hydrogen adsorption/desorption, platinum oxidation, and platinum oxide reduction.¹¹

CV tests of thermally treated TiO_2 were performed to investigate the electrochemical activity of different nanopowders, results of which are shown in Fig. 6. The anodic peak at 0.65 V and cathodic peak at 0.58 V in Fig. 6(a) are associated with the oxidation and reduction of the surface oxide groups. The bigger double layer capacity in P25-700-1000h and P25-700-1100h can be attributed to the formation of TiO_xC_y since surface carbon coating is consumed during annealing, as observed from the TEM images [Fig. 2(b)]. OER was carried out to investigate the catalyst activity toward oxidation of water to generate molecular oxygen in acidic electrolyte medium, $2\text{H}_2\text{O} = 4\text{e}^- + 4\text{H}^+ + \text{O}_2$, and the onset potential for

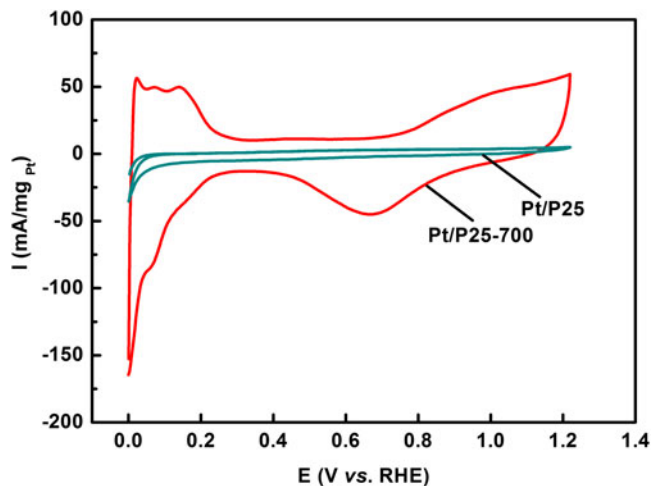


FIG. 5. Cyclic voltammograms of 10 wt% Pt supported on samples P25 and P25-700 in 1 M H_2SO_4 . Much larger currents were observed in the latter sample, which is attributed to the much higher conductivity of the carbon-doped support.

this reaction is a basic criterion to evaluate the efficiency of the catalyst.

According to Nowotny et al.,⁴² the presence of defects at TiO_2 surface, e.g., oxygen vacancies, is essential for water splitting. Undoped TiO_2 showed the worst OER activity, as can be seen in Fig. 6(b). The sample has the highest onset potential and lowest current, which could be attributed to its low surface defects.^{42–44} Introducing carbon doping and further annealing can create oxygen vacancies as predominant defects, as confirmed by the formation

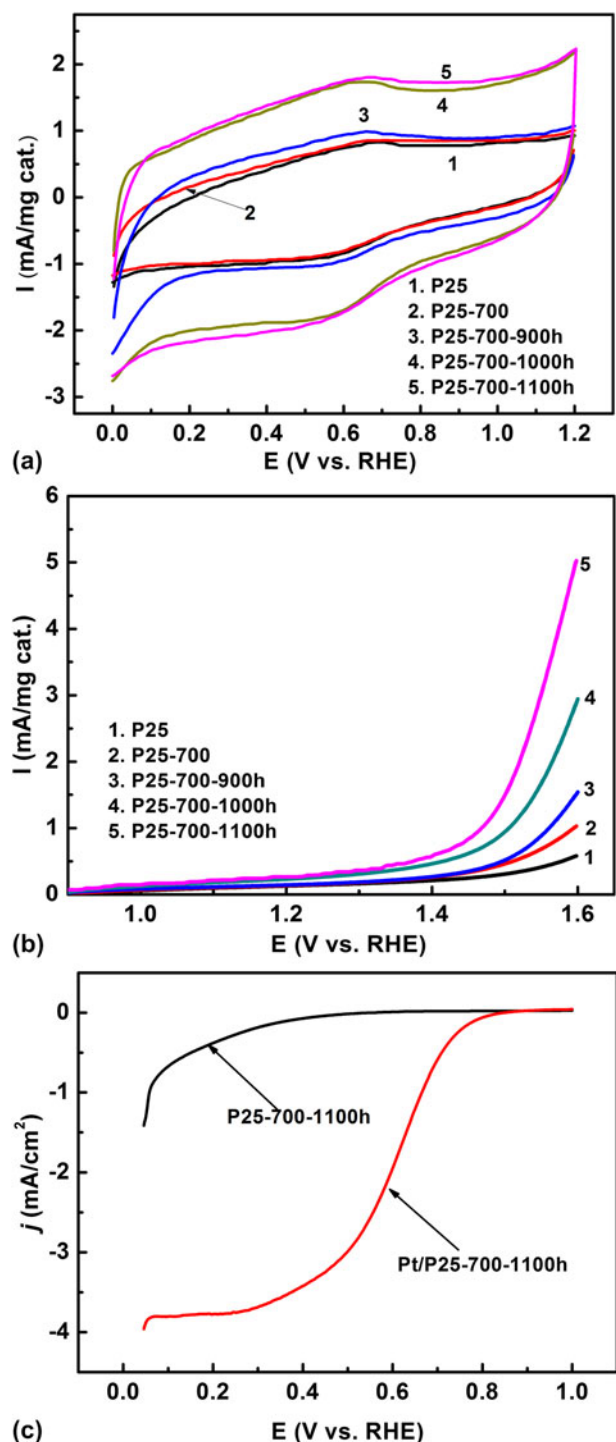


FIG. 6. Electrochemical characterization: (a) cyclic voltammograms of undoped and doped TiO_2 in N_2 -saturated 1.0 M H_2SO_4 with scanning rate at 50 mV/s, (b) OER results of the corresponding nanopowders in N_2 -saturated 1.0 M H_2SO_4 with scanning rate at 5 mV/s. (c) Typical ORR results of TiO_xC_y nanopowders in O_2 -saturated 1.0 M H_2SO_4 with scanning rate at 5 mV/s, with or without Pt electrocatalyst.

of reduced Ti from previous XPS analysis.^{11,14,20,27} Annealed at 1100 °C, the carbon-coated TiO_2 has almost completed the transformation from TiO_2 to TiO_xC_y , which

has the most oxygen vacancies. As a result, the catalyst showed the best OER catalytic activity, with the lowest OER onset potential at 1.45 V.

Many efforts have been made in seeking other oxides to replace the expensive OER catalyst, IrO_2 , which is considered to be the state of the art. Among various candidates, perovskites exhibited comparable or better OER activity than previous reports. Suntivich et al.⁴⁵ most recently reported perovskites with an onset potential in range of 1.5–1.65 V (versus RHE). At 0.4 V overpotential versus RHE (1.23 V), the OER current activities are in a range of 0.12–14 mA/mg_{catal.}. The TiO_xC_y (curve 5) in Fig. 6(b) yielded a ~ 5 mA/mg_{catal.} current density at 1.6 V, therefore, having a comparable OER activity as the reported perovskites and further demonstrating the substantial OER activity of the titanium oxycarbide.

However, none of our samples exhibit ORR activity, as shown in Fig. 6(c), in which large overpotentials and negligible currents were observed. To obtain ORR activity, Pt was deposited on the TiO_xC_y and typical ORR curves⁴⁶ were obtained [Fig. 6(c)]. An onset potential at ~ 0.85 V shows that the TiO_xC_y support is an excellent alternative support to the high surface area carbon black. Altogether, the catalyst Pt/ TiO_xC_y has both OER and ORR activities, demonstrating an effective bifunctional catalyst.

IV. CONCLUSIONS

In this paper, we demonstrated a carbothermal technique that allows making nanoscale TiO_xC_y from commercial TiO_2 P25 nanoparticles. The process is a simple one-step two-stage process. It can be achieved in most lab furnaces under relatively low temperatures. The process involves a carbon coating stage, followed by an annealing stage. By doing so, sintering of the nanoparticles is substantially suppressed, allowing us to maintain the large surface areas of the particles needed for catalyst support. It was found that partial carbon substitution in the TiO_2 lattice occurred at below 1000 °C. But at 1100 °C, the TiO_2 nanoparticles can be completely converted to TiO_xC_y , with only a small increase in particle size. It was also found that markedly improved electronic conductivity can be obtained in TiO_xC_y , which makes it a good substrate for supporting the Pt electrocatalyst. The TiO_xC_y nanopowders obtained showed a significant activity in OER. By depositing Pt on it, a bifunctional catalyst, Pt/ TiO_xC_y , was demonstrated to be effective for both ORR and OER.

ACKNOWLEDGMENTS

The authors would like to thank partial financial support for this research from the U.S. Department of Energy ARPA-E Grant No. DE-AR0000066. We thank Dr. Eric Bohannon for XRD analysis, Mr. Brian Porter for XPS analysis, and Dr. Kai Song for taking TEM images.

REFERENCES

1. J. Newman and W. Tiedemann: Porous-electrode theory with battery applications. *AIChE J.* **21**, 25 (1975).
2. S. Litster and G. McLean: PEM fuel cell electrodes. *J. Power Sources* **130**, 61 (2004).
3. A.L. Dicks: The role of carbon in fuel cells. *J. Power Sources* **156**, 128 (2006).
4. X.L. Wang, H.M. Zhang, J.L. Zhang, H.F. Xu, Z.Q. Tian, J. Chen, H.X. Zhong, Y.M. Liang, and B.L. Yi: Micro-porous layer with composite carbon black for PEM fuel cells. *Electrochim. Acta* **51**, 4909 (2006).
5. S-W. Eom, C-W. Lee, M-S. Yun, and Y-K. Sun: The roles and electrochemical characterizations of activated carbon in zinc air battery cathodes. *Electrochim. Acta* **52**, 1592 (2006).
6. T. Ogasawara, A. Débart, M. Holzapfel, P. Novák, and P.G. Bruce: Rechargeable Li_2O_2 electrode for lithium batteries. *J. Am. Chem. Soc.* **128**, 1390 (2006).
7. A. Débart, J. Bao, G. Armstrong, and P.G. Bruce: An O_2 cathode for rechargeable lithium batteries: The effect of a catalyst. *J. Power Sources* **174**, 1177 (2007).
8. J. Willsau and J. Heitbaum: The influence of Pt-activation on the corrosion of carbon in gas diffusion electrodes—a DEMS study. *J. Electroanal. Chem.* **161**, 93 (1984).
9. S.K. Natarajan and J. Hamelin: Electrochemical durability of carbon nanostructures as catalyst support for PEMFCs. *J. Electrochem. Soc.* **156**, B210 (2009).
10. H. Song, X. Qiu, F. Li, W. Zhu, and L. Chen: Ethanol electro-oxidation on catalysts with TiO_2 coated carbon nanotubes as support. *Electrochem. Commun.* **9**, 1416 (2007).
11. A. Bauer, K. Lee, C. Song, Y. Xie, J. Zhang, and R. Hui: Pt nanoparticles deposited on TiO_2 based nanofibers: Electrochemical stability and oxygen reduction activity. *J. Power Sources* **195**, 3105 (2010).
12. R.E. Fuentes, J. Farrell, and J.W. Weidner: Multimetallic electrocatalysts of Pt, Ru, and Ir supported on anatase and rutile TiO_2 for oxygen evolution in an acid environment. *Electrochem. Solid-State Lett.* **14**, E5 (2011).
13. F.C. Walsh and R.G.A. Wills: The continuing development of Magnéli phase titanium sub-oxides and Ebonex® electrodes. *Electrochim. Acta* **55**, 6342 (2010).
14. X. Li, A.L. Zhu, W. Qu, H. Wang, R. Hui, L. Zhang, and J. Zhang: Magnéli phase Ti_4O_7 electrode for oxygen reduction reaction and its implication for zinc-air rechargeable batteries. *Electrochim. Acta* **55**, 5891 (2010).
15. T. Ioroi, H. Senoh, S-I. Yamazaki, Z. Siroma, N. Fujiwara, and K. Yasuda: Stability of corrosion-resistant Magnéli-phase Ti_4O_7 -supported PEMFC catalysts at high potentials. *J. Electrochem. Soc.* **155**, B321 (2008).
16. W-Q. Han and X-L. Wang: Carbon-coated Magnéli-phase $\text{Ti}_n\text{O}_{2n-1}$ nanobelts as anodes for Li-ion batteries and hybrid electrochemical cells. *Appl. Phys. Lett.* **97**, 243104 (2010).
17. T. Tsumura, N. Kojitani, I. Izumi, N. Iwashita, M. Toyoda, and M. Inagaki: Carbon coating of anatase-type TiO_2 and photoactivity. *J. Mater. Chem.* **12**, 1391 (2002).
18. H. Irie, Y. Watanabe, and K. Hashimoto: Carbon-doped anatase TiO_2 powders as a visible-light sensitive photocatalyst. *Chem. Lett.* **32**, 772 (2003).
19. Y. Choi, T. Umabayashi, and M. Yoshikawa: Fabrication and characterization of C-doped anatase TiO_2 photocatalysts. *J. Mater. Sci.* **39**, 1837 (2004).
20. J.H. Park, S. Kim, and A.J. Bard: Novel carbon-doped TiO_2 nanotube arrays with high aspect ratios for efficient solar water splitting. *Nano Lett.* **6**, 24 (2005).
21. C.A. Grimes and G.K. Mor: *TiO₂ Nanotube Arrays: Synthesis, Properties, and Applications* (Springer Science, Germany, 2009).
22. H.K. Kammler and S.E. Pratsinis: Carbon-coated titania nanostructured particles: Continuous, one-step flame-synthesis. *J. Mater. Res.* **18**, 2670 (2003).
23. Y. Choi, T. Umabayashi, S. Yamamoto, and S. Tanaka: Fabrication of TiO_2 photocatalysts by oxidative annealing of TiC. *J. Mater. Sci. Lett.* **22**, 1209 (2003).
24. M. Inagaki, Y. Hirose, T. Matsunaga, T. Tsumura, and M. Toyoda: Carbon coating of anatase-type TiO_2 through their precipitation in PVA aqueous solution. *Carbon* **41**, 2619 (2003).
25. M. Inagaki, F. Kojin, B. Tryba, and M. Toyoda: Carbon-coated anatase: The role of the carbon layer for photocatalytic performance. *Carbon* **43**, 1652 (2005).
26. M. Toyoda, T. Yano, B. Tryba, S. Mozia, T. Tsumura, and M. Inagaki: Preparation of carbon-coated Magnéli phases $\text{Ti}_n\text{O}_{2n-1}$ and their photocatalytic activity under visible light. *Appl. Catal., B* **88**, 160 (2009).
27. R. Hahn, F. Schmidt-Stein, J. Salonen, S. Thiemann, Y. Song, J. Kunze, V-P. Lehto, and P. Schmuki: Semimetallic TiO_2 nanotubes. *Angew. Chem. Int. Ed.* **48**, 7236 (2009).
28. H.S. Kibombo and R.T. Koodali: Heterogeneous photocatalytic remediation of phenol by platinumized titania-silica mixed oxides under solar-simulated conditions. *J. Phys. Chem. C* **115**, 25568 (2011).
29. J. Lee and W. Choi: Photocatalytic reactivity of surface platinumized TiO_2 : Substrate specificity and the effect of Pt oxidation state. *J. Phys. Chem. B* **109**, 7399 (2005).
30. T. Ioroi, N. Kitazawa, K. Yasuda, Y. Yamamoto, and H. Takenaka: Iridium oxide/platinum electrocatalysts for unitized regenerative polymer electrolyte fuel cells. *J. Electrochem. Soc.* **147**, 2018 (2000).
31. S. Song, H. Zhang, X. Ma, Z-G. Shao, Y. Zhang, and B. Yi: Bifunctional oxygen electrode with corrosion-resistant gas diffusion layer for unitized regenerative fuel cell. *Electrochem. Commun.* **8**, 399 (2006).
32. Y. Xing: Synthesis and electrochemical characterization of uniformly-dispersed high loading Pt nanoparticles on sonochemically-treated carbon nanotubes. *J. Phys. Chem. B* **108**, 19255 (2004).
33. R. Koc and J.S. Folmer: Carbothermal synthesis of titanium carbide using ultrafine titania powders. *J. Mater. Sci.* **32**, 3101 (1997).
34. X. Chen and S.S. Mao: Titanium dioxide nanomaterials: Synthesis, properties, modifications, and applications. *Chem. Rev.* **107**, 2891 (2007).
35. E.A. Reyes-Garcia, Y. Sun, K.R. Reyes-Gil, and D. Raftery: Solid-state NMR and EPR analysis of carbon-doped titanium dioxide photocatalysts ($\text{TiO}_{2-x}\text{C}_x$). *Solid State Nucl. Magn. Reson.* **35**, 74 (2009).
36. Y. Luo, S. Ge, Z. Jin, and J. Fisher: Formation of titanium carbide coating with micro-porous structure. *Appl. Phys. A* **98**, 765 (2010).
37. W. Göpel, G. Rocker, and R. Feierabend: Intrinsic defects of $\text{TiO}_2(110)$: Interaction with chemisorbed O_2 , H_2 , CO, and CO_2 . *Phys. Rev. B* **28**, 3427 (1983).
38. C. Di Valentin, G. Pacchioni, and A. Selloni: Theory of carbon doping of titanium dioxide. *Chem. Mater.* **17**, 6656 (2005).
39. K. Huang, K. Sasaki, R.R. Adzic, and Y. Xing: Increasing Pt oxygen reduction reaction activity and durability with carbon-doped TiO_2 nanocoating catalyst support. *J. Mater. Chem.* **22**, 16824-16832 (2012).
40. J.J. Blackstock, C.L. Donley, W.F. Stickle, D.A.A. Ohlberg, J.J. Yang, D.R. Stewart, and R.S. Williams: Oxide and carbide formation at titanium/organic monolayer interfaces. *J. Am. Chem. Soc.* **130**, 4041 (2008).
41. C. Moreno-Castilla, F.J. Maldonado-Hódar, F. Carrasco-Marín, and E. Rodríguez-Castellón: Surface characteristics of titania/carbon composite aerogels. *Langmuir* **18**, 2295 (2002).

42. J. Nowotny, T. Bak, M.K. Nowotny, and L.R. Sheppard: TiO₂ surface active sites for water splitting. *J. Phys. Chem. B* **110**, 18492 (2006).
43. M. Calatayud, A. Markovits, M. Menetrey, B. Mguig, and C. Minot: Adsorption on perfect and reduced surfaces of metal oxides. *Catal. Today* **85**, 125 (2003).
44. M. Menetrey, A. Markovits, and C. Minot: Reactivity of a reduced metal oxide surface: Hydrogen, water and carbon monoxide adsorption on oxygen defective rutile TiO₂(110). *Surf. Sci.* **524**, 49 (2003).
45. J. Suntivich, K.J. May, H.A. Gasteiger, J.B. Goodenough, and Y. Shao-Horn: A perovskite oxide optimized for oxygen evolution catalysis from molecular orbital principles. *Science* **334**, 1383 (2011).
46. Y. Xing, Y. Cai, M.B. Vukmirovic, W-P. Zhou, H. Karan, J.X. Wang, and R.R. Adzic: Enhancing oxygen reduction reaction activity via Pd–Au alloy sublayer mediation of Pt monolayer electrocatalysts. *J. Phys. Chem. Lett.* **1**, 3238 (2010).